Continuum Resonances in $He^4(p,p')He^{4*}$ †‡

LAWRENCE E. WILLIAMS§
University of Minnesota, Minneapolis, Minnesota
(Received 30 September 1965; revised manuscript received 15 December 1965)

Two resonances are seen in the spectrum of inelastic protons from He^4 with 40-MeV protons incident upon a NTP helium gas target. Resonance I lies at an He^4 excitation energy $E^*=20.46\pm0.14$ MeV and has a c.m. full width $\Gamma_{c.m.}=340\pm40$ keV, while II is at $E^*=22.00\pm0.14$ MeV with $\Gamma_{c.m.}=2.4\pm0.5$ MeV. Data were taken over the range $19\leq E^*\leq24$ MeV at 11 lab angles, $15°\leq\theta\leq90°$, with a 32-detector array of solid-state passing counters mounted in the focal plane of a double-focusing 180° magnetic spectrometer. Angular distributions for the two inelastic groups were obtained through a subtraction of tentative phase space and/or experimental backgrounds. Kinematic limitations prevented following a third broad resonance which appeared at $26\leq E^*\leq28$ MeV.

I. INTRODUCTION

THE purpose of this experiment was to determine the excitation energy E^* of virtual excited states in the He^4 system by inelastic scattering of the Minnesota 40-MeV proton beam from He^4. Previous $He^4(p,p')$ continuum work done at proton bombardment energies $E_p\geq55$ MeV, had indicated a resonance near $E^*=22$–26 MeV,[1–3] several MeV in width, whereas scattering done at $E_p=32$ MeV had shown little structure in the continuum for $E^*\leq23$ MeV.[4] Wickersham[5] was, in fact, able to fit the $He^4+p\rightarrow2p+T$ spectra with a simple phase space plot for $E_p=28$ MeV. Eisberg,[6] using the Minnesota 40-MeV beam, did not find evidence for the broad state and set an upper limit to the cross section for any state having a full width at half-maximum $\Gamma<0.5$ MeV at $E^*\leq28$ MeV:

$$(d\sigma/d\omega)_{He^4(p,p')}\leq1.0\text{ mb/sr}\quad\text{at}\quad\theta=30°. \qquad (1)$$

Thus, until this time, the direct proton excitation of He^4 has shown no more than one resonance. At $E_p=185$ MeV, this peak was explained by a quasi-elastic scattering formalism.[1,7] Such an argument is credible when the beam energy becomes large relative to the 20-MeV binding energy of a single nucleon in He^4. In accordance with the explanation, no resonance had appeared at $E_p<55$ MeV.

The reactions and Q values for the system $p+He^4$ are given in Table I. This experiment is primarily concerned with direct excitation of He^4 states between the onsets of reactions (III) and (V); i.e., $19.0\leq E^*\leq24.0$ MeV and thus includes the broad resonance mentioned above as well as a low-lying continuum state which has appeared in several indirect experiments.

A 20.4-MeV state with $J^\pi=0^+$ and $T=0$ has been inferred by Carl Werntz[8,9] and his co-workers from two quite distinct experiments; that of Poppe *et al.* on the $T(d,np)T$ resonance,[10] and Jarmie *et al.*[11] on $p+T$ elastic scattering. Balashko *et al.*[12] also have demonstrated that the $^1S_0$ phase shift in $T(p,p)T$ exceeds $\frac{1}{2}\pi$ as E_p nears the neutron production threshold (764 keV) and place their corresponding $J^\pi=0^+$ state at $E^*=20.3$ MeV in the He^4 system. Meyerhof[13] has analyzed the Young and Ohlson[14] and Parker *et al.*[15] experiments on 3-body final states in the He^3+d reactions to show that the lower excitation resonance observed is consistent with Werntz's calculation. Recently, Cerny *et al.*[16] have found a 20.1-MeV 0^+ state in He^4 via both the $Li^6(p,He^3)He^4$ and $Li^7(p,\alpha)He^4$ reactions. No direct evidence of this level from $He^4(p,p')$ has been obtained, however.

A third possible region for He^4 excited states that

TABLE I. He^4 reactions and Q values.

Reaction	Q (in MeV)	
$He^4(p,p)He^4$	0	(I)
$He^4(p,d)He^3$	−18.37	(II)
$He^4(p,p\,T)p$	−19.82	(III)
$He^4(p,n\,He^3)p$	−20.58	(IV)
$He^4(p,2d)p$	−23.84	(V)
$He^4(p,pnd)p$	−26.07	(VI)
$He^4(p,2p2n)p$	−28.30	(VII)

† Work supported in part by the U. S. Atomic Energy Commission.
‡ A preliminary account of this work, based upon a thesis submitted to the University of Minnesota in partial fulfillment of the requirements for the degree Doctor of Philosophy, appeared in Phys. Rev. Letters **15**, 170 (1965).
§ Present address: Rutherford High Energy Laboratory P.L.A., Didcot, Berkshire, England.
[1] P. Hillman, A. Johannson, G. Tibell, and H. Tyren, Nucl. Phys. **12**, 596 (1959).
[2] W. Selove and J. Teem, Phys. Rev. **112**, 1658 (1958).
[3] S. Hayakawa *et al.*, Phys. Letters **8**, 330 (1964).
[4] J. Benveniste and B. Cork, Phys. Rev. **89**, 422 (1953).
[5] A. Wickersham, Phys. Rev. **107**, 1050 (1957).
[6] R. Eisberg, Phys. Rev. **102**, 1104 (1956).
[7] Y. Sakamoto, Nuovo Cimento **25**, 565 (1962).
[8] C. Werntz, Phys. Rev. **128**, 1336 (1962).
[9] C. Werntz, Phys. Rev. **133**, B19 (1964).
[10] C. Poppe, C. Holbrow, and R. Borchers, Phys. Rev. **129**, 733 (1963).
[11] N. Jarmie, M. Silbert, D. Smith, and J. Loos, Phys. Rev. **130**, 1987 (1963).
[12] Yu. G. Balashko, I. Barit, L. Dulcova, and A. Kurepin, in *Proceedings of the International Conference on Nuclear Physics, Paris, 1964* (Editions du Centre National de la Recherche Scientifique, Paris, 1965).
[13] W. E. Meyerhof, Bull. Am. Phys. Soc. **10**, 628 (1965).
[14] P. Young and G. Ohlson, Phys. Letters **8**(2), 124 (1964).
[15] P. Parker, P. Donovan, J. Kane, and J. Mollenauer, Phys. Rev. Letters **14**, 15 (1965).
[16] J. Cerny, C. Détraz, and R. Pehl, Phys. Rev. Letters **15**, 300 (1965).

lies somewhat outside the region of interest of this experiment has been examined in photoproton production, $He^4(\gamma,p)T$, and the inverse reaction $T(p,\alpha)\gamma$. In the former case, Fuller[17] found a resonance several MeV in width in the excitation function near $E_\gamma=26$ MeV. The proton angular distribution could be fitted with a simple $\sin^2\theta_{c.m.}$ term (c.m. refers throughout to the center of momentum of the initial reactants), indicating an electric dipole transition. Perry and Bame's[18] inverse-reaction studies, while also revealing a dipole c.m. γ distribution and agreeing with Fuller's cross section at $\theta_{c.m.}=90°$, via detailed balance, showed only a diffuse excitation function maximum near $E_p=4$–5 MeV. Vlasov[19] *et al.*, extending the $T(p,\alpha)\gamma$ experiment to $E_p=7$ MeV and finding the yield curve just beginning to turn over, concluded that their results did not indicate a $J^\pi=1^-$ state in He^4. Sasakawa,[20] however, calculated that a $^1P_1$ state in He^4, which would go to the ground state ($^1S_0$) via an electric dipole transition, is necessary to explain the maximum in photoproton yield at $E^*=26$ MeV. It thus appears probable that at least one electric dipole state occurs between $23\leq E^*\leq 28$ MeV in He^4—although the evidence is by no means unequivocal.

In resume, we should note that a $J^\pi=0^+$ continuum state at $E^*=20.1$–20.4 MeV with $\Gamma<0.5$ MeV is relatively well established by this time. A second broader resonance some 1.2 MeV higher in excitation seen by Parker *et al.*[15] and by Cerny *et al.*[16] might be correlated with the $E^*=22$–23-MeV peak seen in $He^4(p,p')$. Cerny *et al.*,[16] however, believe that still a third state, the analog of the Li^4 ground state at $E^*=22.5\pm0.3$ MeV, is the one which corresponds to the $He^4(p,p')$ broad resonance. This would make the 22-MeV state in He^4 a $T=1$ level. The quasi-elastic scattering formalism, of course, makes the excited-state interpretation of the single inelastic proton resonance a bit suspect.

A final region of interest lies between $24\leq E^*\leq 28$ MeV where a $^1P_1$ state in He^4 seems to have been demonstrated by photoproton production.

II. EXPERIMENTAL EQUIPMENT

A. Beam Optics

The 40-MeV proton beam was drifted through the unexcited third tank of the Linac and, via a pair of doublet magnetic quadrupole lenses, brought to a focus at the object point of a 40 in. radius, uniform field, 60° sector magnet. By rotating both object and image-side pole faces of the 60° magnet and thus changing the angle between the optic axis and the perpendicular to the pole face,[21] both axial (along the field) and radial (perpendicular to the field) image focusing was obtained. The 60° sector's optic-axis energy was determined absolutely to within ±100 keV by a floating wire technique. The 0.25 in. diameter collimator at the sector image point limited E_p variations to about ±60 keV for a nominally 40-MeV beam.

The inelastically scattered protons from He^4 were bent in a vertical plane by a 40 in. radius, 180°, double-focusing magnetic spectrometer and detected in a linear array of 32 surface-barrier passing counters mounted in the spectrometer focal plane. The focal plane had been determined experimentally and was found to lie at an angle of 62±2° with respect to the vertical exit face of the spectrometer and in such a way that higher energy particles are focused at a greater distance. The spectrometer average optic-axis field was absolutely determined, using the known beam energy, by $H(p,p)H$ scattering at an appropriate angle. The charged-particle identification was done by pulse-height analysis of each counter output, comparing the voltage pulses to those produced by p-p scattering at the same field. The optical-axis momentum p_0 is then $e_0B_0\rho_0/c$, with B_0 being the field at the optic axis radius ρ_0. Thus, with a knowledge of the beam energy and the scattered particle's energy and mass, a direct determination of the excitation energy E^* in He^4 was obtained. It should be noted that in the angular range $15°\leq\theta\leq 90°$ and excitation range $19\leq E^*(He^4)\leq 24$ MeV of the experiment, only the ground-state deuterons of reaction II at $\theta=90°$ were of appropriate magnetic rigidity and intensity to make separation of inelastic protons difficult. Hence at this angle, a 5-mil Mylar foil was used instead of the regular 1-mil chamber exit foil to strip the deuterons from the scattered beam. A plan view of the beam optics system is shown in Fig. 1.

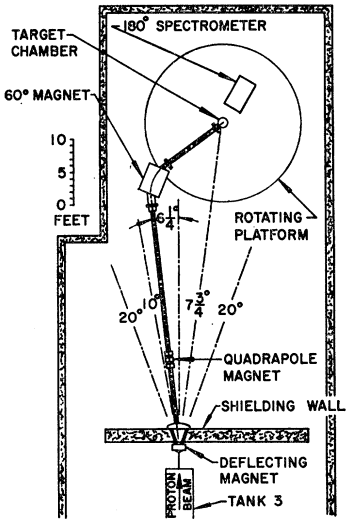

FIG. 1. Beam-handling system layout.

[17] E. Fuller, Phys. Rev. **96**, 1306 (1954).
[18] J. Perry and S. Bame, Phys. Rev. **99**, 1368 (1955).
[19] N. A. Vlasov, S. P. Kalinin, A. A. Ogloblin, L. N. Samoilov, V. A. Sidorov, and V. I. Chuev, Zh. Eksperim. i Teor. Fiz. **28**, 639 (1955) [English transl.: Soviet Phys.—JETP **1**, 500 (1955)].
[20] T. Sasakawa, Progr. Theoret. Phys. (Kyoto) **22**, 595 (1959).
[21] W. Cross, Rev. Sci. Instr. **22**, 717 (1951).

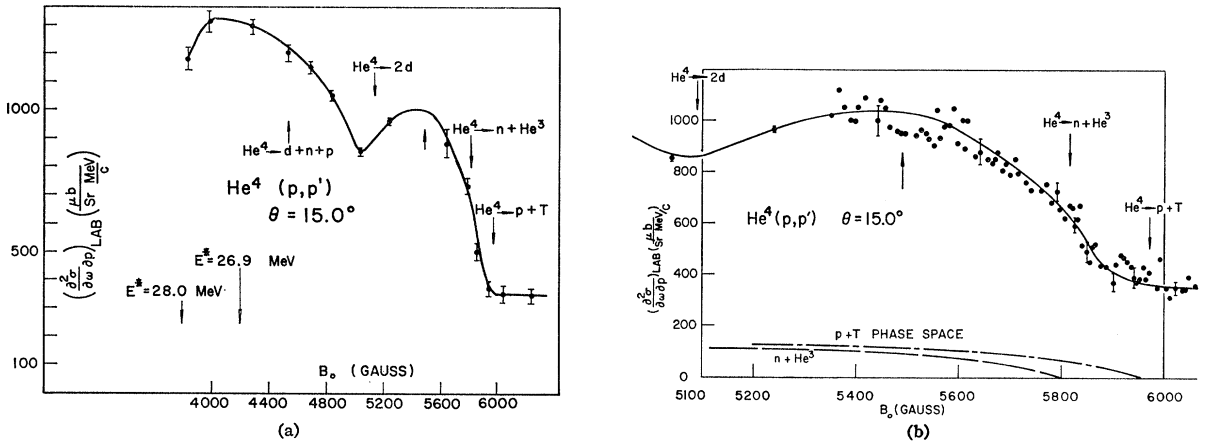

FIG. 2. (a) Extended inelastic-proton-momentum spectrum at $\theta=15°$. (b) Expanded inelastic-proton-momentum spectrum near p+T threshold at $\theta=15°$.

B. Target

The target was a 12 in. diameter cylindrical vessel with thin foils separating the NTP helium from both the beam-transport vacuum system and the spectrometer vacuum system. The He^4 gas was in continuous flow at a positive pressure of 1 in. of H_2O or less above atmospheric to preclude outgassing or residual air contamination. A barograph and thermometer showed pressure and temperature variations of the target to be neglibible. The target-out curve shown in Fig. 6 at $\theta=60°$ demonstrates that the target-out background in the region of interest is structureless. As a final check, a spectrum taken with NTP air in the chamber at $\theta=60°$ also revealed no continuum resonances in the magnetic-field region corresponding to $20\leq E^*\leq 22$ MeV. The target thickness seen by the spectrometer was 0.68 in. $\csc\theta$, which corresponds to an area density of 0.29 $\csc\theta$ mg/cm^2. The kinematic spread of the outgoing inelastic protons due to finite angular acceptance of the spectrometer was, at most, ± 90 keV. The full width at half-maximum (FWHM) of the Landau spread of the incoming beam was, typically, 100 keV while the exiting inelastic protons generally had a Landau FWHM of 50 keV. The calculated total experimental FWHM, excluding the intrinsic width of any virtual state, was on the order of 180 keV.

C. Beam Monitors

An internal Faraday cup immersed in the target was used for the initial data. The arrangement was felt to be somewhat unsatisfactory because of the necessarily small size of the cup and because of the possibility of current flow between collecting electrode and ground through the ionized He^4 gas path in the target. This was remedied by using an external cup with a diffusion-pump vacuum system and having both permanent magnets and a biased repeller ring to inhibit secondary electron emission. The large size of this external cup required that a monitor counter be used for $\theta\leq 25°$, since at smaller angles the spectrometer rotation was obstructed by the cup. A small plastic-scintillator monitor counter was used with satisfactory results. The consistency of the collected charge (S) measurements was good throughout and will be discussed shortly.

D. Electronics

The negative pulses from individual inelastic protons passing through the surface-barrier diodes were preamplified in the experimental area and post-amplified in the counting room. Each signal was then fed to a discriminator-biased inverter circuit which had two functions: (1) to generate a routing pulse for signals above the lower bias limit (discriminator function) and (2) to invert the signal and bias off the inherent diode noise and low-energy background (biased inverter function). Positive pulses from all 32 detectors were then mixed, amplitude-analyzed, and stored in the appropriate group of 32 channels in the memory of a 1024-channel pulse-height analyzer. The group address was provided by the routing pulse.

E. Data Analysis and Calculations

The 32 diodes occupy a momentum range of only $\pm 0.02=\Delta p_0/p_0$. Overlapping spectrometer field runs were therefore necessary to cover the required He^4 excitation range at fixed θ. Independent of θ or p_0, each diode has a known constant radial size Δx and fixed solid angle $\Delta\omega$. Thus, we experimentally determine $(\partial^2\sigma/\partial\omega\partial x)_i$ directly by recording the counts n_i in the ith diode when S/e_0 incident protons strike the He^4 target of atomic density, $t\csc\theta$ nuclei/cm^2. Explicitly,

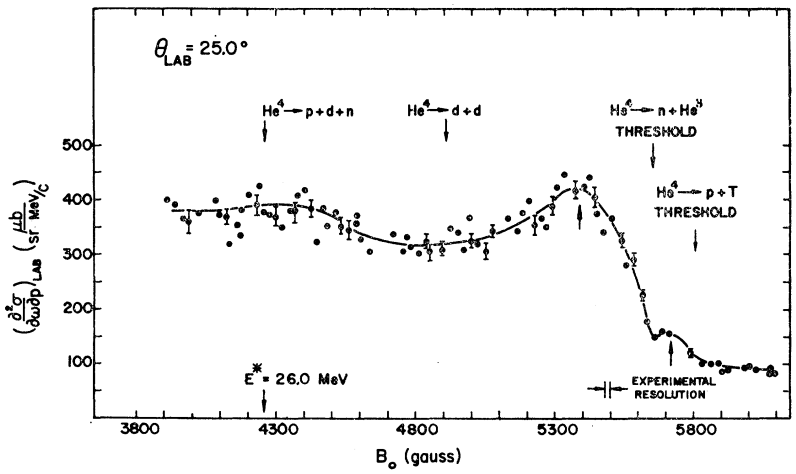

FIG. 3. Inelastic proton momentum spectrum at $\theta=25°$. (The unmarked vertical arrows indicate the spectrometer field values of the resonances in this and the other $\partial^2\sigma/\partial\omega\partial p_0$ graphs.)

we set

$$\left[\frac{\partial^2\sigma(\theta,p_0)}{\partial\omega\partial x}\right]_i=\frac{n_i}{(S/e_0)}\left(\frac{1}{t}\right)\frac{\sin\theta}{\Delta\omega\Delta x}. \tag{2}$$

By Judd's[22] first-order theory:

$$\Delta x=W_\beta(\Delta p_0/p_0)\rho_0, \tag{3}$$

where the momentum dispersion W_β was empirically found to be 3.92 ± 0.10 near $B_0=6600$ G by elastic scattering from He^4 at $\theta=100°$. This is consistent with the value $W_\beta=4$ predicted for an "$n=\frac{1}{2}$" field. Combining (2) and (3) we have

$$\left[\frac{\partial^2\sigma(\theta,p_0)}{\partial\omega\partial p_0}\right]_i=\frac{W_\beta}{p_0}\left[\frac{\partial^2\sigma(\theta,p_0)}{\partial\omega\partial x}\right]_i\rho_0. \tag{4}$$

The $\sin\theta$ term in Eq. (2) is the calculated lowest order geometry factor for our gas target–spectrometer system. The correctness of this factor as well as the empirical determination of the term $t\Delta\omega$ was checked to within $\pm5\%$ by normalizing 40 MeV He^4 elastic scattering taken with this system to the previous data of Brussel and Williams[23] at the same beam energy.

The total relativistic lab energy of the detected particle of rest mass m_0 is given by

$$E_0=\gamma\gamma_{c.m.}(1+\beta\beta_{c.m.}\cos\theta_{c.m.})m_0c^2, \tag{5}$$

where the subscript c.m. refers to quantities measured in the center of momentum frame[24] of He^4+p and $\beta=(1-\gamma^{-2})^{1/2}$ is the speed (units of c) of this frame relative to the lab. The quantity $\gamma_{c.m.}$ depends upon the effective[25] mass M recoiling at $\pi-\theta_{c.m.}$[26]:

$$\gamma_{c.m.}=\frac{(\mathcal{E}/c^2)^2+m_0^2-M^2}{2m_0(\mathcal{E}/c^2)}, \tag{6}$$

where $\mathcal{E}$ is the *total* energy relative to the c.m. frame. In a three- or more-body final state with masses m_0, m_1, $\cdots$, m_J, $M\geq\sum_{i=1}^{J}m_i$. When a resonance appears in such a system, the observed inelastic proton continuum exhibits a peak at a spectrometer field B_0 corresponding to a particular M in Eq. (6). Subtracting the rest energy of He^4 from Mc^2 gives E^* of the resonance. In practice, the calculation was carried out by a Control Data 1604 computer which varied the recoiling mass M so as to reproduce the observed resonance spectrometer field values.

To interpret any experimental momentum peaks, a lowest order perturbation-theory calculation of $(\partial^2\sigma/\partial\omega\partial p_0)$, the inelastic-proton-momentum spectrum, must be carried out for three-body final states. The relativistic result is[27]

$$\left(\frac{\partial^2\sigma}{\partial\omega\partial p_0}\right)_{c.m.}\propto(k)^{1/2}(p_0^2)_{c.m.}\left\{\frac{6(\mathcal{E}-E_0)_{c.m.}^2}{c^2}\times\left[\frac{(m_1^2+m_2^2)c^2}{D}-\frac{(m_1^2-m_2^2)^2c^4}{D^2}\right]+4k\left[D+\frac{2(\mathcal{E}-E_0)_{c.m.}^2}{c^2}\right]\right\} \tag{7}$$

with

$$4k=1-2(m_1^2+m_2^2)c^2/D+(m_1^2-m_2^2)^2c^4/D^2$$

and

$$D=(\mathcal{E}-E_0)^2_{c.m.}/c^2-(p_0^2)_{c.m.}.$$

The only unknown proportionality constant in Eq. (7) is the perturbation matrix element between initial $(p+He^4)$ and final three-body states, $\mathfrak{M}_{if}$ (m_1,m_2). In the phase-space calculation, $\mathfrak{M}_{if}$ was assumed to be independent of $\theta_{c.m.}$ and E_0. The appropriate Jacobian was used to transform the calculated c.m. inelastic momentum spectra into the lab frame of reference at

[22] D. Judd, Rev. Sci. Instr. **21**, 213 (1950).
[23] M. Brussel and J. Williams, Phys. Rev. **106**, 286 (1957).
[24] $\beta_{c.m.}=(1-\gamma_{c.m.}^{-2})^{1/2}$.
[25] In a two-body final state M is just the recoiling mass.
[26] J. D. Jackson, *Classical Electrodynamics* (John Wiley & Sons, Inc., New York, 1962), p. 402.
[27] M. Block, Phys. Rev. **101**, 796 (1956).

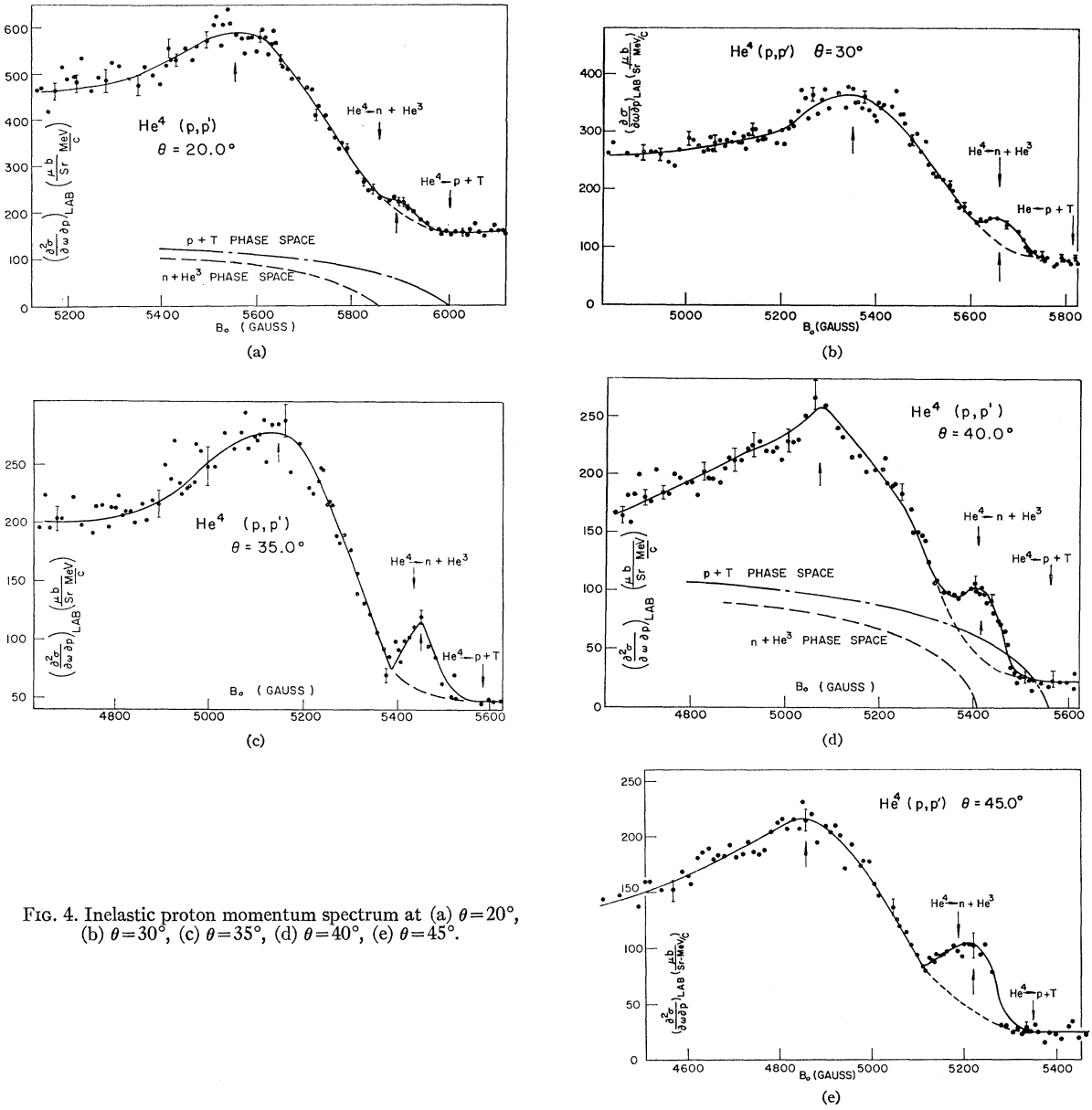

FIG. 4. Inelastic proton momentum spectrum at (a) $\theta=20°$, (b) $\theta=30°$, (c) $\theta=35°$, (d) $\theta=40°$, (e) $\theta=45°$.

angle θ. Resultant graphs of $\partial^2\sigma/\partial\omega\partial p_0$ for reactions III and IV, labeled $p+T$ and $n+He^3$ phase space, respectively, were plotted along with experimental momentum spectra in Figs. 2, 4, and 7. For convenient comparison, $\mathfrak{M}_{if}$(III) was equated to $\mathfrak{M}_{if}$(IV) for these plots.

III. RESULTS AND ERRORS

A. Momentum Spectra

Lab measurements of $\partial^2\sigma/\partial\omega\partial p_0$ were made between $\theta=15°$ and 45° inclusively in 5° steps as well as at $\theta=52°$, 60°, 75°, and 90°. In these results, Figs. 2 through 7, the titled arrows indicate the calibrated spectrometer field values for the onsets of various reactions given in Table I while unlabeled arrows mark resonances in the momentum spectra. At a given angle, a background independent of He^4 excitation energy appears at B_0 values corresponding to excitation below the onset of $He^4\rightarrow p+T$. This flat continuum is made up of two major parts: (1) uncharged particles coming from the collimators and Faraday cup and (2) elastically scattered protons which have been energy degraded by the internal spectrometer baffles. The rapid increase in the latter, as the scattering angle was decreased, resulted in the lower angular limit of 15°.

At all lab angles except 15°, where the elastic background became prohibitive, two inelastic-proton resonances were observed between the onsets of reactions III and V. The peaks are not explicable by means of

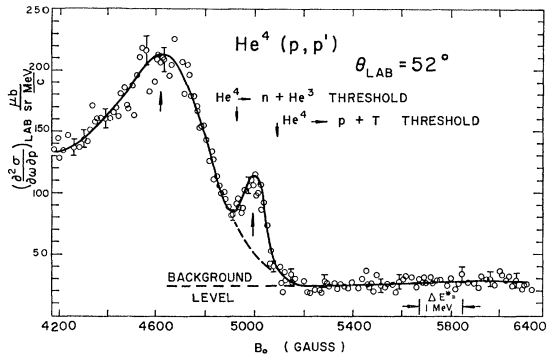

FIG. 5. Extended inelastic proton momentum spectrum at $\theta=52°$.

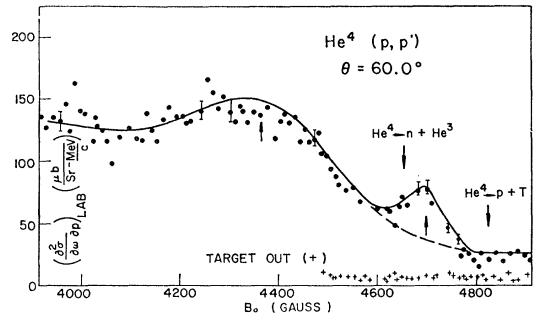

FIG. 6. Inelastic proton momentum spectrum (target out run included) at $\theta=60°$.

the lowest order phase-space calculations as Eq. (7) yields only the relatively smooth $\partial^2\sigma/\partial\omega\partial p_0$ curves plotted for the p+T and n+He³ channels. It should be noted that the experimental $\partial^2\sigma/\partial\omega\partial p_0$ curves were simply drawn by eye within the constraints of the individual error bars attached to the data points and do not represent any sort of "most probable" fit. The errors shown are relative, typically ±4%, and primarily caused by the statistical uncertainty in the number of counts.

The absolute $\partial^2\sigma/\partial\omega\partial p_0$ errors are calculated to be about ±9%, owing to the additional ±5% uncertainties in the normalization of the elastic data and in the elastic data themselves.

B. Resonance Masses

The resonances were assumed to correspond to two-body final states with the one unknown mass calculated by Eqs. (5) and (6). Consistent He⁴ excitation energies of 20.46±0.14 and 22.0±0.14 MeV were then found for peaks I and II, respectively. A 140-keV rms measured variation in E^* seems consistent with the known beam energy uncertainty of ±60 keV and typical spectrometer calibration errors of ±20 G. The B_0 indeterminacy alone corresponds approximately to a ±100-keV error in Mc^2.

At $\theta=15°$, the extended spectrum [Fig. 2(a)] taken up to $E^*=28$ MeV exhibits a possible third resonance at $26\leq E^*\leq 28$ MeV. An additional indication of this peak is seen in the $\theta=25°$ extended spectrum shown in Fig. 3. A bound state search below the He⁴ → p+T threshold at $\theta=52°$ is shown in Fig. 5 down to $E^*=15$ MeV. No statistically significant peaks on the $\partial^2\sigma/\partial\omega\partial p_0$ spectrum were seen between $15\leq E^*\leq 19.8$ MeV at this angle. Moreover, at all angles, the continua were experimentally flat within statistics, down to 1 MeV or so below the onset of the p+T reaction.

C. Angular Distributions

The uncertainty in the numerical value of the matrix elements $\mathfrak{M}_{if}$ for both the p+T and n+He³ channel breakup of He⁴ precluded any theoretical continuum (3-body) subtraction from peaks I and II. In addition, an experimental flat background is present throughout. For the relatively weak first resonance (I), it was possible to take into account both effects by means of the dashed curve drawn under this peak in each momentum spectrum. The difference between $\partial^2\sigma/\partial\omega\partial p_0$ and the dashed background curve for peak I exhibited a Gaussian shape centered about M_Ic^2 at all angles. This Gaussian result was then integrated over momentum to yield $(d\sigma/d\omega)_I$ which, when transformed to the c.m. frame, has the form shown in Fig. 8. The

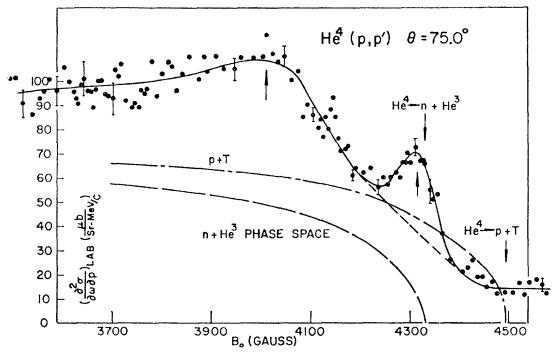

(a)

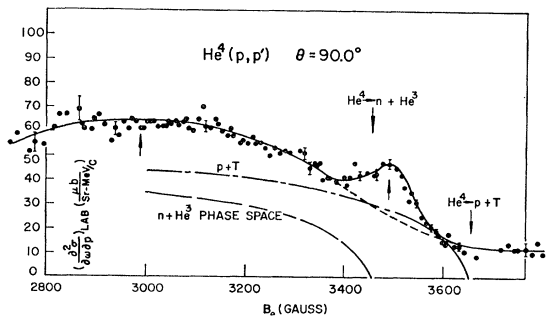

(b)

FIG. 7. Inelastic proton momentum spectrum at (a) $\theta=75°$, (b) $\theta=90°$.

error bars, generally about $\pm 10\%$, are relative and were defined by the accuracy of the subtraction. The absolute errors are $\pm 15\%$ due to normalization uncertainties. Several data points are shown at some angles with the open circles representing internal Faraday cup runs and other symbols indicating external cup or counter beam monitoring. No systematic charge errors appeared in either the angular distributions or in a direct comparsion of $\partial^2\sigma/\partial\omega\partial p_0$ spectra taken under different cup conditions.

Peak II, being both more intense and broader than I at all lab angles, does not lie upon any obvious background representative of phase space. An integration over the inelastic proton momentum spectrum to obtain the differential cross section for this state is consequently more difficult than for the narrow resonance. In the approximate calculation of $(d\sigma/d\omega)_{c.m.}$ of state II plotted in Fig. 9, we have set the differential cross section for the broad resonance equal to the area of a triangle whose height and width were made proportional to the height above flat background and FWHM, respectively, of the broad $\partial^2\sigma/\partial\omega\partial p_0$ peak. The relative uncertainty in this technique increases with θ since, at larger angles, the p+T and n+He^3 phase space factors constitute a larger fraction of the experimental inelastic proton momentum spectra [see Figs. 2(b) and 7(b)]. We estimate an average relative uncertainty of $\pm 20\%$ in this differential-cross-section calculation. The error wings shown in Fig. 9 represent only the $\pm 5\%$ relative uncertainty in the area of the triangles due to the experimental errors in the $\partial^2\sigma/\partial\omega\partial p_0$ measurement.

D. Intrinsic FWHM (Γ) of the Resonances

The sum of the calculated momentum variances (standard deviation squared) due to the several experimental sources of proton-momentum uncertainty; e.g., beam energy changes, kinematics ($\Delta\theta$), Landau momentum spread in target and foils, and spectrometer current fluctuations, was added to an unknown term corresponding to the intrinsic width of a state and the total of these equated to the total experimental variance of a given $\partial^2\sigma/\partial\omega\partial p_0$ peak. For the narrow virtual state, a measured total momentum variance was taken from the Gaussian $\partial^2\sigma/\partial\omega\partial p_0$ peak resulting from a subtraction of the dashed background curve shown in each momentum spectrum. The total experimental variance of the broad state was directly measured from the inelastic proton momentum spectra with only the flat background being subtracted. In either case, the FWHM for the state was computed from its intrinsic variance assuming a Gaussian $\partial^2\sigma/\partial\omega\partial p_0$ distribution. The mean c.m. frame values for FWHM (Γ) of both states are given, along with typical errors, in Table II.

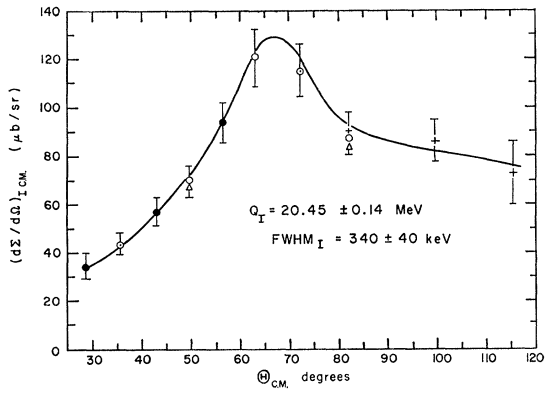

FIG. 8. Angular distribution of state I in c.m. frame.

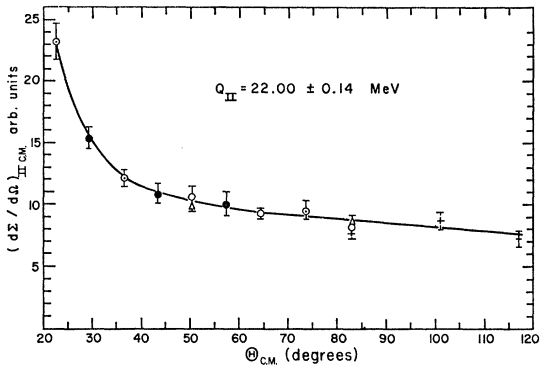

FIG. 9. Angular distribution of state II in c.m. frame (arbitrary units).

TABLE II. Summary of resonance parameters. [The full widths at half-maximum (Γ's) are in the c.m. frame.]

State	$E^*(He^4)$	$\Gamma(FWHM)_{c.m.}$
I	20.46±0.14 MeV	340 ±40 keV
II	22.00±0.14 MeV	2.4± 0.5 MeV

IV. CONCLUSIONS

Resonance I, seen at $E^*=20.46\pm0.14$ MeV with the relatively narrow $\Gamma_{c.m.}$ of 340 ± 40 keV, probably is the first direct inelastic experimental evidence for the 20.4-MeV state calculated by Werntz[8,9] and Meyerhof[13] to be $J^\pi=0^+$ and $T=0$. Our $(d\sigma/d\omega)_I$ satisfies Eisberg's limit, Eq. (1). Peak II at $E^*=22.00\pm0.14$ MeV with $\Gamma_{c.m.}=2.4\pm0.5$ MeV would appear to be the broad resonance seen previously at higher beam energies.[1–3] Since the total kinetic energy relative to the center of momentum is only 32 MeV in this experiment, the argument for II being an example of quasi-elastic scattering may be somewhat weakened. From the tenative c.m. angular distribution of II, Fig. 9, it appears to have a quite different spin and/or parity assignment than resonance I, Fig. 8. A model of the $He^4(p,p')He^{4*}$ interaction is needed, however, to determine J^π or T from our angular distributions.

The association of resonance II with other experimental observations is somewhat ambiguous at present.

Meyerhof[28] has shown that a p-wave interaction is consistent with a resonance at $E^*=21$–22 MeV seen in $He^4(e,e')$ [29] and $D(He^3,2p)T$.[15] Cerny *et al.*[16] believe that a $T=1$ analog to their broad Li^4 ground-state resonance, existing in He^4 at 22.5 ± 0.3 MeV, is, because of its breadth and excitation energy, the broader one we see via $He^4(p,p')$. A general reduction of all pertinent data to the He^4 system seems to be necessitated by the lack of agreement between peak energies and widths as seen in various experiments.[16]

The third resonance, which has started to appear at $26\leq E^*\leq 28$ MeV cannot be followed because of the kinematic and background limitations of this experiment. It may correspond to the $T=1, J^\pi=1^-$ $He^4(\gamma,p)T$ resonance seen previously.[17] No earlier $He^4(p,p')$ experiment has shown structure at this level. Selove and Teem[2] did find a single broad resonance near $E^*=26$ MeV with $E_p=95$ MeV, but felt this was the same resonance as the 22-MeV excitation peak seen at Uppsala.[1] A higher resolution, high-energy bombardment of He^4 is necessary to explore this state.

The absence of any structure just below the $p+T$ threshold puts an estimated upper limit of about 10% of $(d\sigma/d\omega)_I$ on any bound state whose width $\Gamma<0.5$ MeV; i.e., the maximum such cross section is on the order of 10 μb/sr for $19.0\leq E^*\leq 19.8$ MeV.

[28] W. E. Meyerhof, Rev. Mod. Phys. **37**, 512 (1965).
[29] R. Frosch, R. Rand, M. Yearian, H. Crannell, and L. Suelzle, Phys. Letters **19**, 155 (1965).

ACKNOWLEDGMENTS

The author would like to thank his advisor, Professor J. H. Williams. Professor N. M. Hintz deserves my special acknowledgment for his ingenious counsel in the design and use of experimental equipment.

Jerry Gaughran developed the electronics of the 32-diode arrangement and kept the system in excellent operating condition. John Benjamin, Dave Madland, and Vladimir Shkolnik assisted in running the experiment and taking the data. Dick Hendricks, John Anderson, and Walt Ekman aided and effected the mechanical designs. Bob Featherstone, Dennis Olson, and Walt Schwartz maintained the Linac to produce the high-intensity beam required for this experiment.